united nations
educational, scientific
and cultural
organization

international atomic
energy agency

the
abdus salam
international centre for theoretical physics

Course on "Inverse Methods in Atmospheric Science"
1 - 12 October 2001

301/1332-16

"Deriving Aerosol Properties from Lidar Signals"

G.P. GOBBI
Istituto per L'Inquinamento Atmosferico CNR
Rome, Italy

Please note: These are preliminary notes intended for internal distribution only.

Course on "*Inverse Methods in Atmospheric Sciences*"
International Centre for Theoretical Physics – Trieste, October 2001

DERIVING AEROSOL PROPERTIES FROM LIDAR SIGNALS

Gian Paolo Gobbi

Istituto per l'Inquinamento 'Atmosferico CNR – Rome –ITALY
(gobbi@ifa.rm.cnr.it)

This two-hour lecture will cover the fundamentals of the lidar (laser radar) technique and will introduce methods of signal analysis to derive aerosol properties from single-wavelength lidar traces. In particular, the first point will be addressed by:

1) A Lidar technique primer:

1.1 What is a lidar
1.2 Components of lidar systems
1.3 Scattering in the atmosphere
1.4 What can be observed by lidar
1.5 The lidar equation and its solution

Aerosols and their scattering properties will then be introduced in part two:

2) Backscatter and extinction

2.1 Atmospheric aerosols and their climatic impact
2.2 Build-up of aerosol backscatter and extinction
2.3 Wavelength dependence of refractive index
2.4 Wavelength dependence of backscatter
2.5 Depolarization of lidar signals
2.6 Orthogonal cross-section coordinates

Finally, actual analysis of the lidar signal will be addressed:

3) Deriving aerosol properties by lidar

3.1 Correcting lidar traces for aerosol extinction
3.2 A model of aerosol extinction/backscatter ratio
3.3 Determining aerosol physical properties from lidar traces
3.4 Effects of particles non-sphericity

Lidars operate by sending laser pulses into the atmosphere and collecting the backscattered light by means of telescopes provided with highly sensitive photodetectors.

Analysis of the signal intensity then allows a range-resolved inference of the physical and chemical properties of the scattering media (S).

Principal components of a lidar system:

Emitter: Pulsed lasers (from UV to IR). Nd-YAG, Ruby, Alexandrite, Ti-Sa, Diode, etc.;

Receiver: Optical telescopes. From single lens (0.01 m^2) to multiple-mirror (10 m^2);

Bandpass: Interference filters ($\Delta\lambda$ 0.1-10 nm), monocromators, interferometers, etc.;

Detector: Photomultipliers (UV-NIR), Avalanche photodiodes (IR) (10^5-10^7 current gain);

Signal acquisition: A/D conversion, Photon counting (10-100 Mhz sampling rate or bandpass capability); (S)

Typical laser beam divergence of 1 mrad generates spots of 1 m at 1 km and of 10 m at 10 km.

Considering that typical range resolution is 10-100 m the resulting lidar sampling volume is very small;

High laser repetition rates (10-100 Hz) allow for short term averaging (seconds);

These characteristics allow to study atmospheric processes ranging from the micro to the macro scale.

Similarly to radars, the return time of the laser pulse (dt) indicates the distance (R) of the scattering object: $R = c\,dt/2$

Typical laser wavelengths of the order of one micron (0.001 mm), permit good detection of objects of similar size. In fact, elastic backscattering is quite efficient in this case

Therefore, lidars are ideal instruments to remotely observe aerosol and thin clouds, which are made of particles of size ranging between hundredths and tens of microns.

Lidars also detect atmospheric gases.

In fact:

- Rayleigh scattering allows for good definition of the atmospheric molecular density (and consequently temperature) up to z≈100 km; (S T)
- Differential absorbtion allows for detection of trace gases as Ozone, Water vapor, Sulfur dioxide etc. at several kilometers from the system; (S dial)
- Raman scattering allows for definition of atmospheric density, temperature and of trace gases concentration (H_2O, SO_2, CO_2, etc.) (S raman)

This series of lectures shall focus onto the lidar detection of aerosols and clouds.

The scientific interest in the study of these two atmospheric constituents is due to their role in controlling the planet climate.

In fact, one of the global effects of clouds is to cool the planet by reflecting back to space part of the incoming solar radiation. Overall, aerosol too reflect solar radiation. It is estimated that the cooling effect of aerosols is approximately 1/30th of the cloud-induced one. Since the atmospheric burden of anthropogenic aerosols is steadily growing, their radiative and cloud-modifing effects keep growing too.

Volcanic aerosols too tend to cool the planet. These particles form in the stratosphere following gas and particle injection by major eruptions.
Due to its vertical stability, volcanic aerosols remain in the stratosphere for years, producing a global, long lasting cooling of some tenths of a degree.

One of the major unknowns about atmospheric aerosols is their altitude distribution. Lidars represent the best way to reduce such uncertainty.

The Lidar Equation:

$$E(\lambda, R) = E_L \bullet (c\,\tau_d/2) \bullet (A_0/R^2) \bullet \xi(\lambda) \bullet \beta(\lambda, R) \bullet T^2(R)$$

...describes the amount of energy reaching the lidar detector from the distance R, and during the integration time interval τ_d, which in turn defines the lidar profile range resolution: $dR = c\,\tau_d / 2$

E_L : Laser pulse energy;
R : Range;
A_0 : Area of lidar receiver (telescope);
$\xi(\lambda)$: Receiver spectral transmission;
c : Speed of light;
$\beta(\lambda, R)$: Volume backscatter coefficient;
$T(\lambda, R)$: Atmospheric transmittance

The two variables carrying the geophysical information we want to retrieve are: $\beta(\lambda, R)$: the volume backscatter coefficient, and $T(\lambda, R)$, the Atmospheric transmittance

The volume backscatter coefficient of a species x being:

$$\beta_x(\lambda, R) = N_x(R) \bullet d\sigma_{sx}(\lambda, \theta) / d\Omega$$

where N_x and $d\sigma_{sx}(\lambda, \theta) / d\Omega$ represent the volume number concentration and the differential scattering cross section (at θ = 180°), respectively.

In the case of elastic backscatter from the atmosphere, $\beta(\lambda, R)$ can be expressed as:

$$\beta_{m+a}(\lambda, R) = \beta_m(\lambda, R) + \beta_a(\lambda, R)$$

where the subscripts "m" and "a" stand for the molecular and the aerosol (particulate) component, respectively. In fact, an aerosol-free atmosphere is only found above an altitude of about 30 km.

The atmospheric transmittance between the lidar site (R=0) and the range R can be expressed as:

$$T(\lambda, R) = e^{-\int_0^R \sigma(\lambda, R)\,dR}$$

Where $\sigma(\lambda, R)$ is the atmospheric extinction coefficient:

$$\sigma_x(\lambda, R) = N_x(R)\,\sigma_{xs}(\lambda)$$

with $\sigma_{xs}(\lambda)$ the species extinction cross section.

Again, in an atmosphere composed of molecules and aerosols we can express σ as:

$$\sigma_{m+a}(\lambda, R) = \sigma_m(\lambda, R) + \sigma_a(\lambda, R)$$

Solving the lidar equation:

By omitting the range and wavelength-dependence symbols and assuming the receiver spectral transmittance to be $\xi(\lambda)$=1 we obtain:

$$E = E_L \cdot \frac{c\tau_d}{2} \cdot \frac{A_0}{R^2} \cdot (\beta_m + \beta_a) \cdot e^{-2\int_0^R (\sigma_m + \sigma_a) dR}$$

This equation contains the two unknowns β_a and σ_a (β_m and σ_m are either measured or modeled). To be solved it needs some relationship linking the two variables. Collis and Russell (1976) indicated as a general approximation the following one:

$$\beta_a = \text{cost}\ \sigma_a^g$$

with g depending on the specific properties of the scattering medium and generally spanning the range 0.67<g<1. Several versions of this relationship have been used in literature (Klett, 1985; Kovalev, 1993)

Klett (1985) showed that a good retrieval of backscatter from the lidar measurement can only be obtained if a functional relationship, $\beta_a = f(\sigma_a)$, not a fixed one, is employed. We shall see later how the relationship between β and σ can be determined.

One of the most popular solutions of the lidar equation is the analytical one described by Klett (1985):

$$\beta^a(R) + \beta^m(R) = \frac{\exp(S^a - S^c)}{\frac{1}{\beta_c} + 2\int_{R_c}^{R} \exp(S^a - S^c) dR}$$

This is a stable solution, however, it contains the functional relationship $B_a = f(\sigma_a) = \beta_a / \sigma_a$ which forces an iterative process to retrieve the correct value of β_a (β_m is derived either from air density measurements or models).

This solution has been found by defining the range corrected signal:

$$S(R)=\ln\left[E(R)\cdot R^2/\tau_d\right]$$

which converts the lidar equation into:

$$\frac{dS}{dR}=\frac{1}{\beta_{m+a}}\frac{d\beta_{m+a}}{dR}-2\sigma_{m+a}=\frac{1}{\beta_{m+a}}\frac{d\beta_{m+a}}{dR}-\frac{2\beta_{m+a}}{B_a}+2\beta_m\left(B_a^{-1}-B_m^{-1}\right)$$

By defining now the new signal variable S':

$$S'-S'_c=S-S_c+\frac{2}{B_m}\int_R^{R_c}\beta_m dR'-2\int_R^{R_c}\frac{\beta_m}{B_a}dR'$$

the latter becomes:

$$\frac{dS'}{dR}=\frac{1}{\beta_{m+a}}\frac{d\beta_{m+a}}{dR}-\frac{2\beta_{m+a}}{B_a}$$

which is solved by the Klett equation after definition of the boundary values at $R=R_c$, the calibration range ($R< R_c$).

A few useful formulas about cross sections:

The differential backscatter cross section of the "average" air molecule (below 100 km) [Hinkley, 1976]:

$$d\sigma_m(\lambda,\pi)/d\Omega = 5.45\,[\lambda(\mu m)/0.55]^{-4}\times 10^{-28}\ cm^2\ sr^{-1}$$

Notice the characteristic λ^{-4} dependance of the scattering.
At sea level (typical molecular density $N_m=2.5\times10^{19}\ cm^{-3}$) this leads to:

$$\beta_m(\lambda,0) = [\lambda(\mu m)/0.55]^{-4}\times 1.39\times 10^{-8}\ cm^{-1}\ sr^{-1}$$

From the Rayleigh scattering theory, the extinction/backscatter ratio of air molecules is:

$$\sigma_m/\beta_m = 4\pi/1.5 = 8.378$$

(S cross sect)

The volume backscatter coefficient $\beta(\lambda, R)$ and extinction coefficient $\sigma(\lambda, R)$ are the atmospheric backscatter and extinction cross sections per unit volume of air:

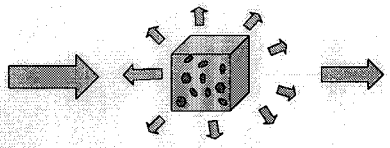

Therefore, they are expressed in units of:

$$\beta\ [cm^2\ sr^{-1}/cm^3] = [cm^{-1}\ sr^{-1}]$$

$$\sigma\ [cm^2/cm^3] = [cm^{-1}]$$

Tabella.ppt

Backscattering from particles:

The Mie theory is the most common tool employed to compute scattering properties of atmospheric particles. It describes the scattering of spherical particles with size comparable to the incident wavelength. It applies well to liquid aerosols, cloud and fog droplets. It has drawbacks in the case of solid (dust, smoke) aerosols and ice crystals.

The Mie backscatter coefficient of a size distribution $N_a(r)$ of spherical particles is:

$$\beta_a(\lambda)=\int_0^\infty \sigma_B(r,\lambda,m)\cdot N_a(r)dr$$

where σ_B is the Mie backscatter cross section, and r and $m=n-ik$ represent the particle's radius and complex refractive index, respectively.

In the following sections these properties will be described in detail.

The "Mie" backscatter cross section $\sigma_b(r, \lambda, m)$ can be written as:

$$\sigma_B(r,\lambda,m)=\pi r^2 Q_B(x,m)$$

where $Q_b(x, m)$ is the backscatter efficiency, provided as a solution of e.m. scattering by Mie(e.g. Kerker [1969]). $Q_b(x, m)$ is a complex function of particles refractive index and of the "Mie" parameter:

$$x = 2\pi r/\lambda$$

In a similar fashion, the "Mie" extinction cross section $\sigma_E(r, \lambda, m)$ can be written:

$$\sigma_E(r,\lambda,m)=\pi r^2 Q_E(x,m)$$

where $Q_E(x, m)$ is the extinction efficiency. Q_B and Q_E are expressed by an infinite series of Riccati-Bessel functions of x and mx. Some examples of the dependence of Q_B on x and mx are reported *hereafter* (S) :

To compute backscatter and/or extinction coefficients of a distribution of particles N(r) (cm^{-3}) the product $\sigma_B N(r)$ ($cm^2\ sr^{-1}\ cm^{-3} = cm^{-1}\ sr^{-1}$) must be integrated over r:

$$\beta_a=\int_0^\infty Q_B\pi r^2 N(r)dr$$

One of the most popular analytical formulations of size distributions is the log-normal one:

$$N(r)=\frac{dn}{d\log r}=\frac{N}{\sqrt{2\pi}\log\sigma}\exp\left[-\frac{(\log r-\log r_m)^2}{2\log^2\sigma}\right]$$

where r_m and σ *stand for* the distribution modal radius and width, respectively. This function has been shown to reproduce pretty well the bell-shaped dispersion of natural aerosols.

The build-up of aerosols backscatter can then be illustrated by the following (S) :

Backscatter and depolarization ratio

A common way to present lidar data (and avoid dealing with the several orders of magnitude range of lidar signals) is the backscatter ratio:

$$R_B = (\beta_a + \beta_m) / \beta_m$$

Laser light is often polarized. Polarization results to be an useful tool to investigate aerosol phase (liquid vs. solid, i.e., droplets vs. crystals): In fact, spheres do not introduce any depolarization when backscattering a polarized beam. Conversely, non-spherical particles depolarize part of the incident polarized light they backscatter.

The common way to quantify depolarization of lidar signals is the depolarization ratio:

$$D = S_{\perp} / S_{//}$$

where $S_{\perp}$ and $S_{//}$ represent the lidar signal detected on polarization planes perpendicular and parallel to the laser one, respectively.

Therefore, polarization lidars need to operate two detection channels.

Depolarization induced by air molecules does not exceed 1%. This is theoretically quantified and explained as due to their non-symmetrical structure [Young, 1980].

A theoretical description of lidar depolarization from particles of size comparable to the wavelength is still rather qualitative. In fact, analytical solutions are obtained only for particles with an axis of symmetry, i.e., rather regular ones, e.g., Toon et al., [1990], Mishchenko et al., [1997]. (S)

Actual observations show a consistent "saturation" in the depolarization at D=50%, generated by simple solid particles (ice crystals, desert dust). (S)

Such behavior allows for inference of the aerosol phase (S)

Aerosols and climate

As previously mentioned, the scientific interest in the study of aerosols is due to their role in controlling the planet climate. In fact, aerosols scatter and absorb solar radiation and provide cloud condensation sites. The model-simulated effects of aerosols on climate tend to counterbalance green-house warming [e.g., Charlson, 1995] (S)

However, some indetermination still exists on the sign of the effects (warming or cooling) of absorbing particles as desert dust. We need to remember that desert dust is the second contributor (after marine) to the global aerosol load. (S)

Radiative effects of desert dust strongly depend on aerosol altitude, a poorly known parameter [Liao, 1998].

This situation explains the interest in studying desert dust and marine aerosol by lidar:

The extinction/backscatter relationship for desert dust and marine aerosols:

To quantitatively invert the lidar signal a model has been developed to explore and parameterize this extinction/backscatter relationship R_{eb}.

The approach of this model is simple [Barnaba and Gobbi, 2001] (S3λ):

1) look at the variability of R_{eb} observed in nature;
2) determine dispersion and behavior of these relationships;
3) fit the resulting data by analytical curves (usually polynomials in log-log coordinates);

SOME CONCLUSIONS:

LIDARs provide an efficient technique to observe atmospheric minor constituents with high spatial and temporal resolution;

Remote-sensing of the atmosphere necessitates the synergic contribution of active and passive techniques, operating both from space and from the ground;

During the next decades LIDAR applications will conquer a large share of the global remote sensing activities;

LIDAR applications and retrievals still represent an open field, offering stimulating opportunities to young scientists.

REFERENCES:

A list of over 600 lidar-related papers can be found at the www site: http://www.osa.org/HOMES/GENERAL/BIBLIO/lidar97.htm

Barnaba, F, and G. P. Gobbi, Lidar estimation of tropospheric aerosol extinction, surface area and volume: Maritime and desert dust cases, J. Geophys. Res., 106, 3005-3018, 2001.

Charlson, R. J. (Ed.) Aerosol forcing of climate, J. Wiley, 416pp, New York, 1995.

d'Almeida, G., P Koepke, and E. P. Shettle, Atmospheric aerosols, 561 pp., A Deepack, Hampton, VA, 1991.

Hinkley, E. D. (Ed.), Laser monitoring of the atmosphere, Springer Verlag, 380pp, New York, 1976.

Kerker, M., The scattering of light and other electromagnetic radiation, Acad. Press, New York, 1969

Klett, J. D., Lidar inversion with variable backscatter/extinction ratios, Applied Optics, 24, 1638-1643, 1985.

Kovalev, V. A., Lidar measurement of the vertical aerosol extinction profiles with range-dependent backscatter to extinction ratio, Applied Optics, 30, 6053-6065, 1993.

Liao, H., and J.H. Seinfeld, Radiative forcing by mineral dust aerosols: Sensitivity to key variables, J. Geophys. Res., 103, 31637-31645, 1998.

Measures, R. M., Laser Remote Sensing, J. Wiley, New York, 510 pp., 1984.

Mishchenko, M. I. et al., Modeling phase functions for dustlike tropospheric aerosols using a shape mixture of randomly oriented polydisperse spheroids, J. Geophys. Res., 102, 16,831-16,847, 1997.

Toon, O. B., E. V. Browell, S. Kinne and J. Jordan, An analysis of lidar observations of polar stratospheric clouds, Geophys. Res. Lett., 17, 393-396, 1990.

Young, A. T., Revised depolarization corrections for atmospheric extinction, Appl. Opt., 19, 3247-3248, 1980.

Lidar-related Web Sites:

LIDAR REFS.: http://www.osa.org/HOMES/GENERAL/BIBLIO/lidar97.htm
LIDAR DIRECTORY: http://www-rab.larc.nasa.gov/lidar

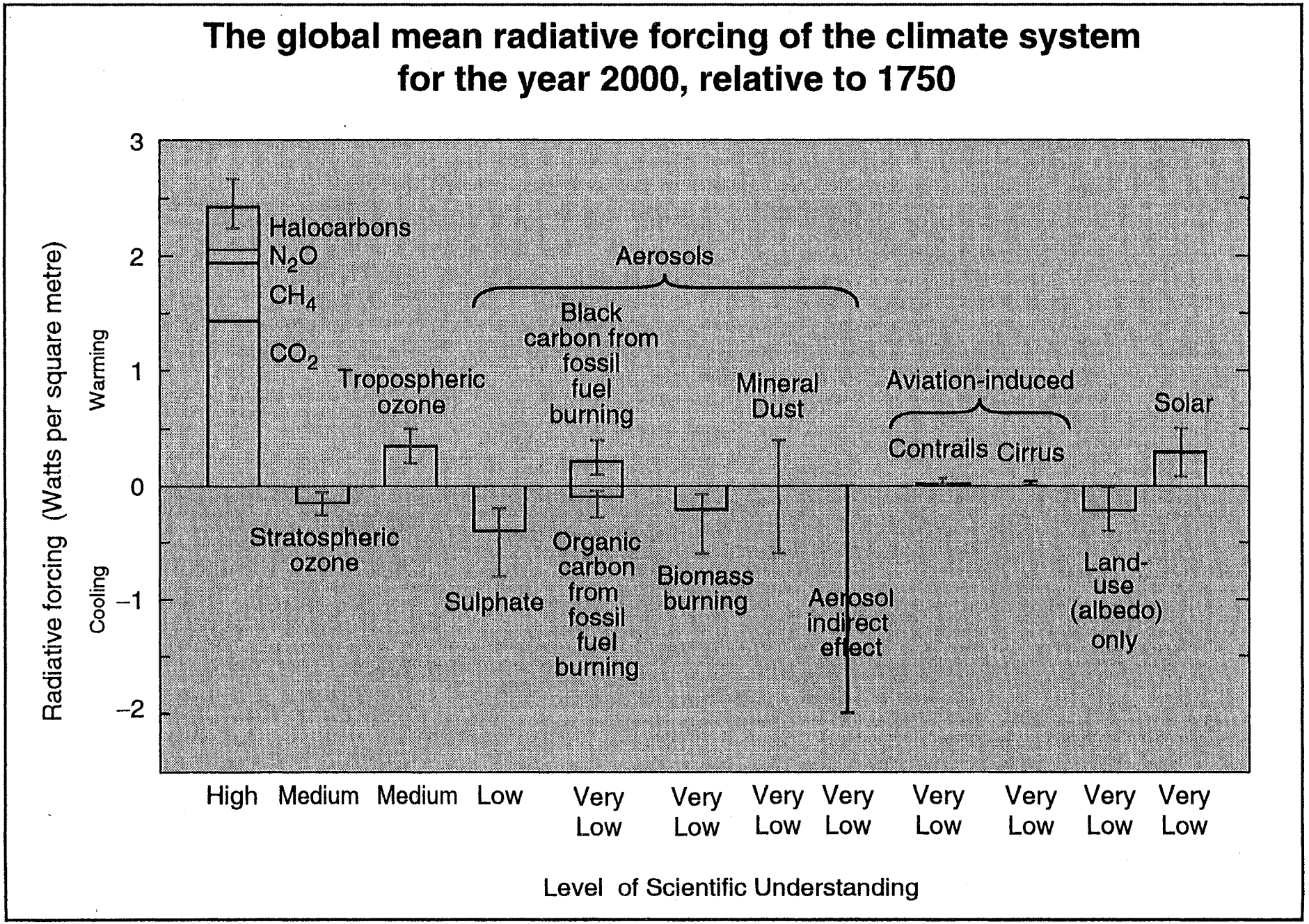

Figure 3: Many external factors force climate change.

ATMOSPHERIC AEROSOLS EXHIBIT BOTH MULTIMODAL AND MULTICOMPONENT CHARACTERISTICS; THAT IS :

Each atmospheric parcel can contain aerosols differing in:

- NATURE (refractive index);
- SHAPE (liquid ones are spherical solid ones are not);
- SIZE DISTIBUTION (usually multimodal, that is each aerosol type can present several modes);

Such variability extends both to the horizontal, vertical and temporal dimensions.

INVERTING PHYSICAL PROPERTIES OF AEROSOLS FROM EITHER ACTIVE OR PASSIVE RADIOMETRIC MEASUREMENTS IS THEREFORE A HARD TASK

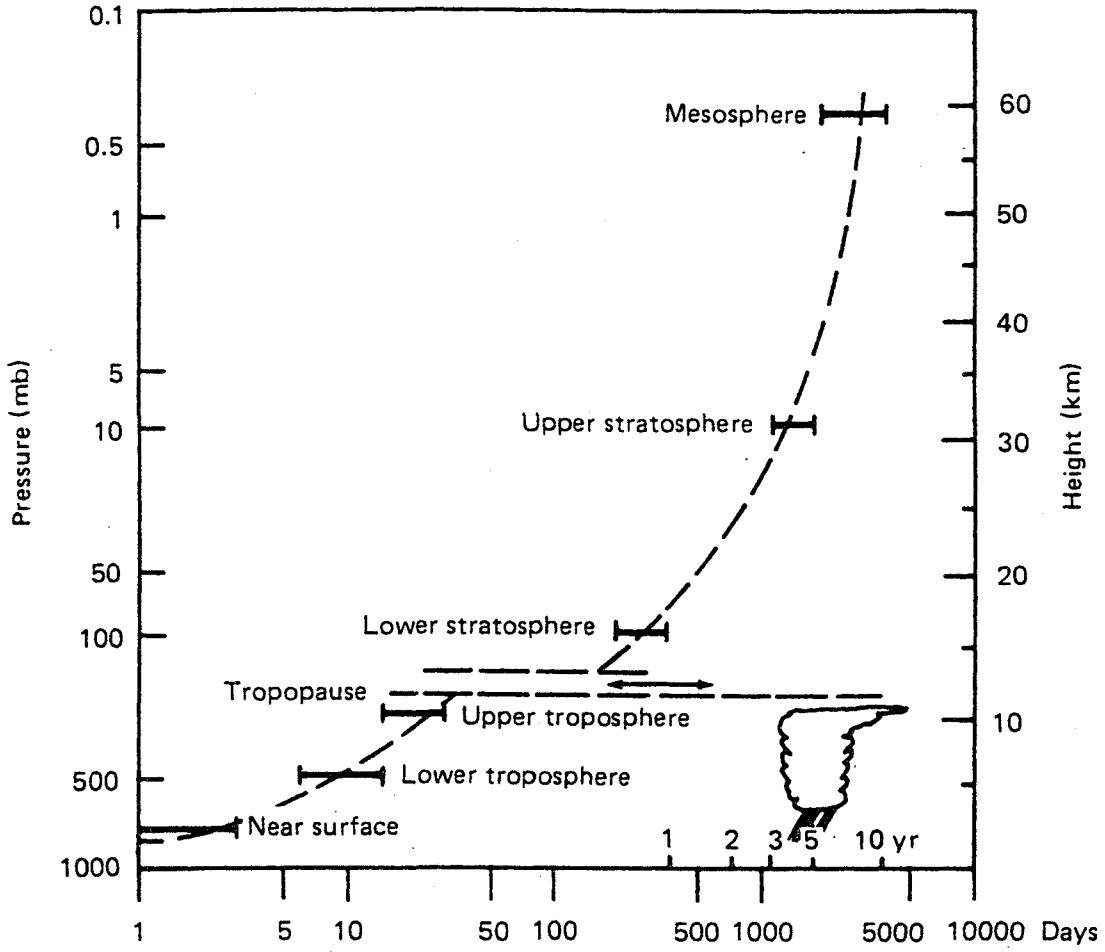

Figure 6.16. Mean residence times of aerosols as a function of height. The double-headed arrow between the two tropopause height limits (horizontal dashed lines) indicates uncertainty in lifetimes in this height regime. From Bach (1976).

Two important reactions would be (Shimazaki and Whitten, 1976):

$$H + NO_2 \longrightarrow HO + NO \qquad (k = 2.97(10^{-11})\ cm^3\ s^{-1}) \qquad (6.3)$$

$$H + O_3 \longrightarrow HO + O_2 \qquad (k = 2.60(10^{-11})\ cm^3\ s^{-1}) \qquad (6.4)$$

The formation of sulfuric acid would then proceed principally by (Davis, 1974):

$$2HO + SO_2 \longrightarrow H_2SO_4 \qquad (6.5)$$

In reaction (6.5) the HO molecules are supplied by reactions (6.3) and (6.4), and the SO_2 presumably comes up from the ground. A number of other reactions are available for depleting H (Shimazaki and Whitten, 1976), but their reaction rates (k) are all much slower than those for (6.3) and (6.4). Some of the HO molecules from these two reactions might combine with ozone to yield $HO_2 + O_2$ with a rate of $1.7(10^{-14})\,cm^3\,s^{-1}$, but the HO_2 would also oxidize sulfur dioxide to produce H_2SO_4 (Davis, 1974).

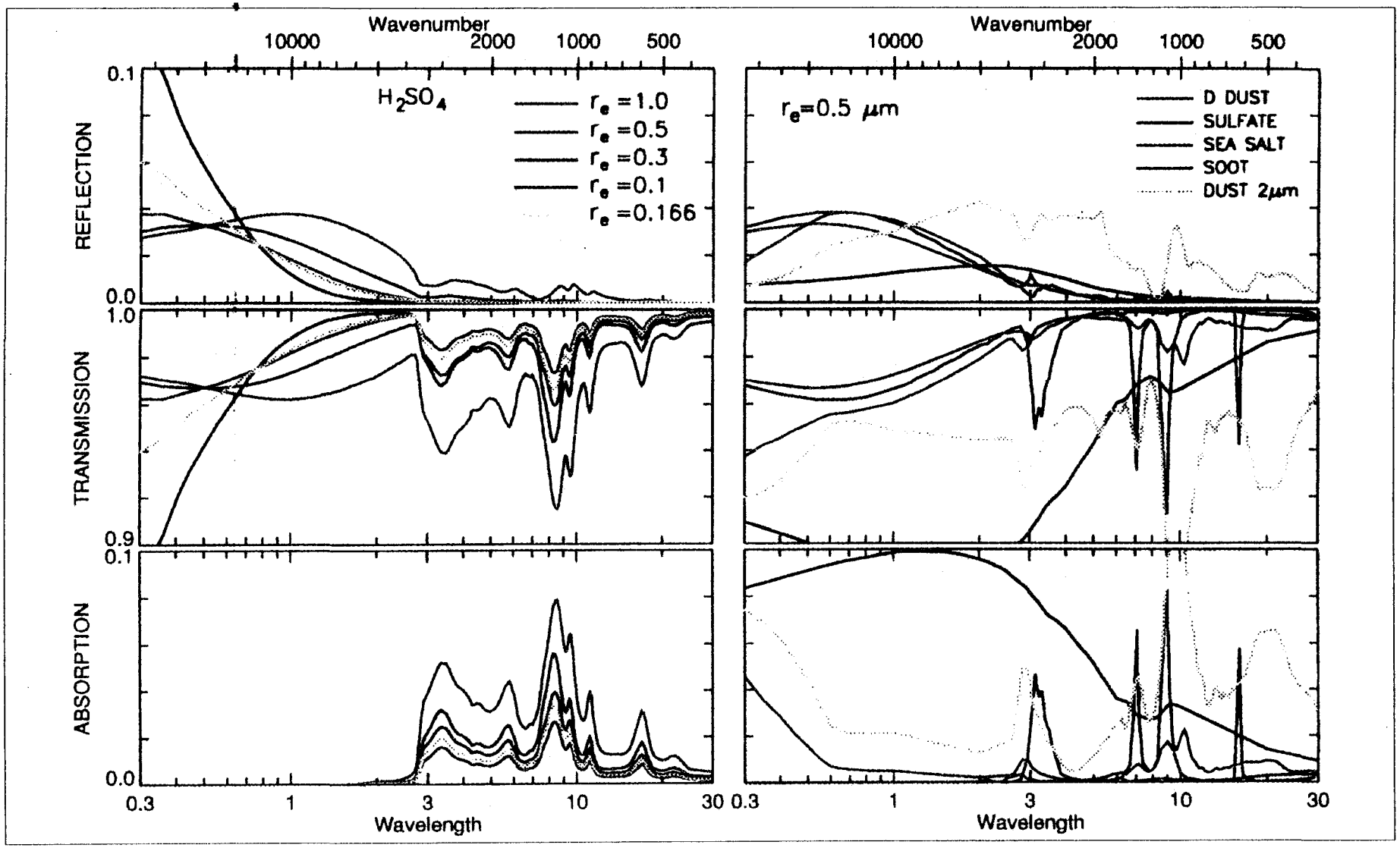

Plate 2.5 Globally integrated radiative properties for H_2SO_4 (left) and representative tropospheric aerosols (right) calculated for $\delta = 0.1$.

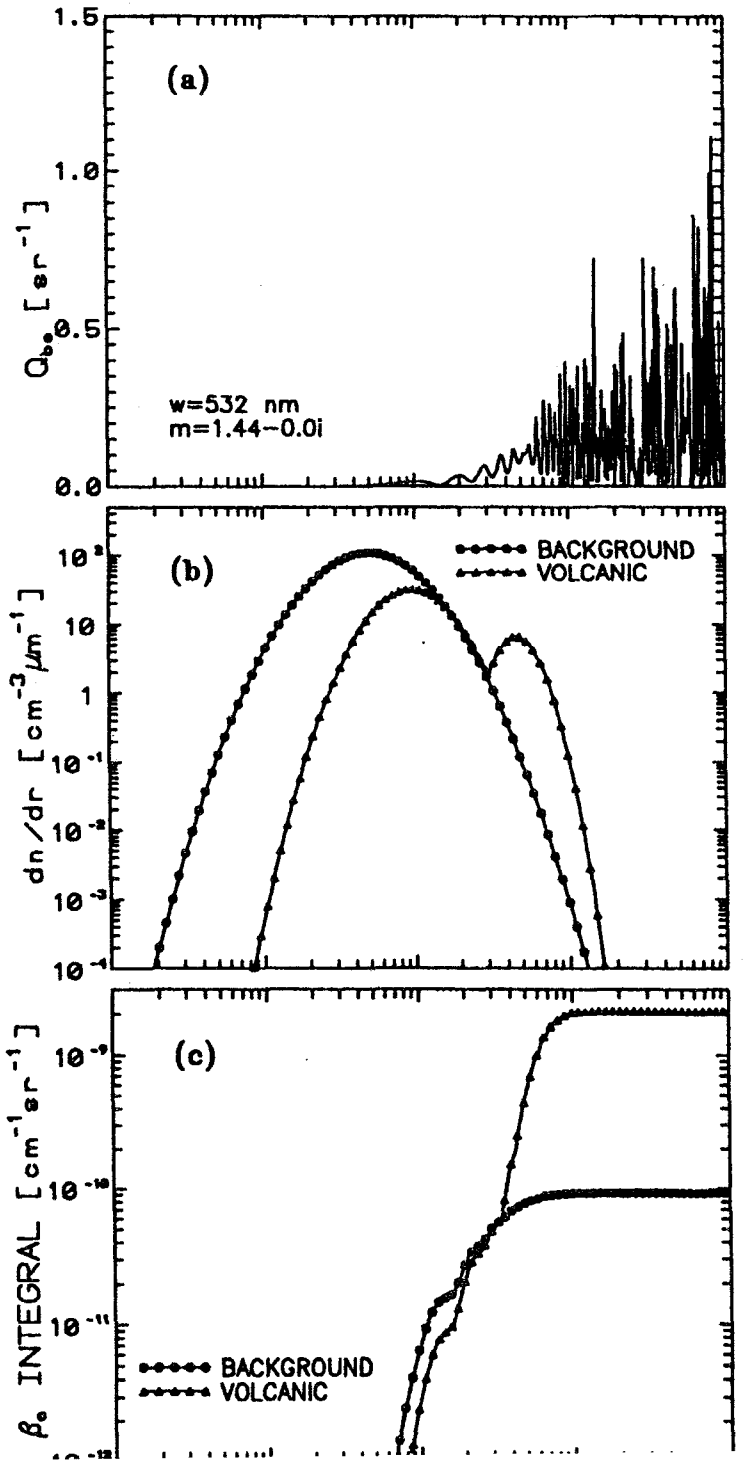
(a)
w=532 nm
m=1.44−0.0i
Q_{ext} [sr^{-1}]
(b)
BACKGROUND
VOLCANIC
dn/dr [cm^{-3} μm^{-1}]
(c)
BACKGROUND
VOLCANIC
β_e INTEGRAL [cm^{-1}sr^{-1}]

Fig. 1

Remember that at each observed wavelength the lidar equation is underdetermined because of the presence of the β_a and σ_a terms.

Combination of the width of the size distribution and absence of marked spectral features in the operational range of lasers (UV-NIR) does not allow to implement DIAL techniques for aerosol retrieval.

One technique used to obtain aerosol extinction together with backscatter adds a Raman N_2 channel to the laser central wavelength one. In this case σ_a is obtained at a shifted (~20-40 nm) wavelength and measurements are only possible at night.

To keep the lidar system small and portable and to operate in daylight we are developing a different approach:

- Employ single wavelength, polarization systems
- Develop model relationships to link β_a and σ_a for various classes of aerosols

BUILD-UP OF ERROR ON LIDAR-RETRIEVED AEROSOL BACKSCATTER COEFFICIENT, β_a

$$d\beta_a / \beta_a \approx dS/S + dN_{mol} / N_{mol} + d\tau /2$$

	Magnitude
dS/S (range-dependent)	0.01-0.5
$d N_{mol} / N_{mol}$	0.005-0.05
$d\tau/2$ (range and aerosol dependent)	0.005-0.3

Typical variability range (near-far range) = **0.02-0.85**

Near range = 100 m
Far range = 15 km

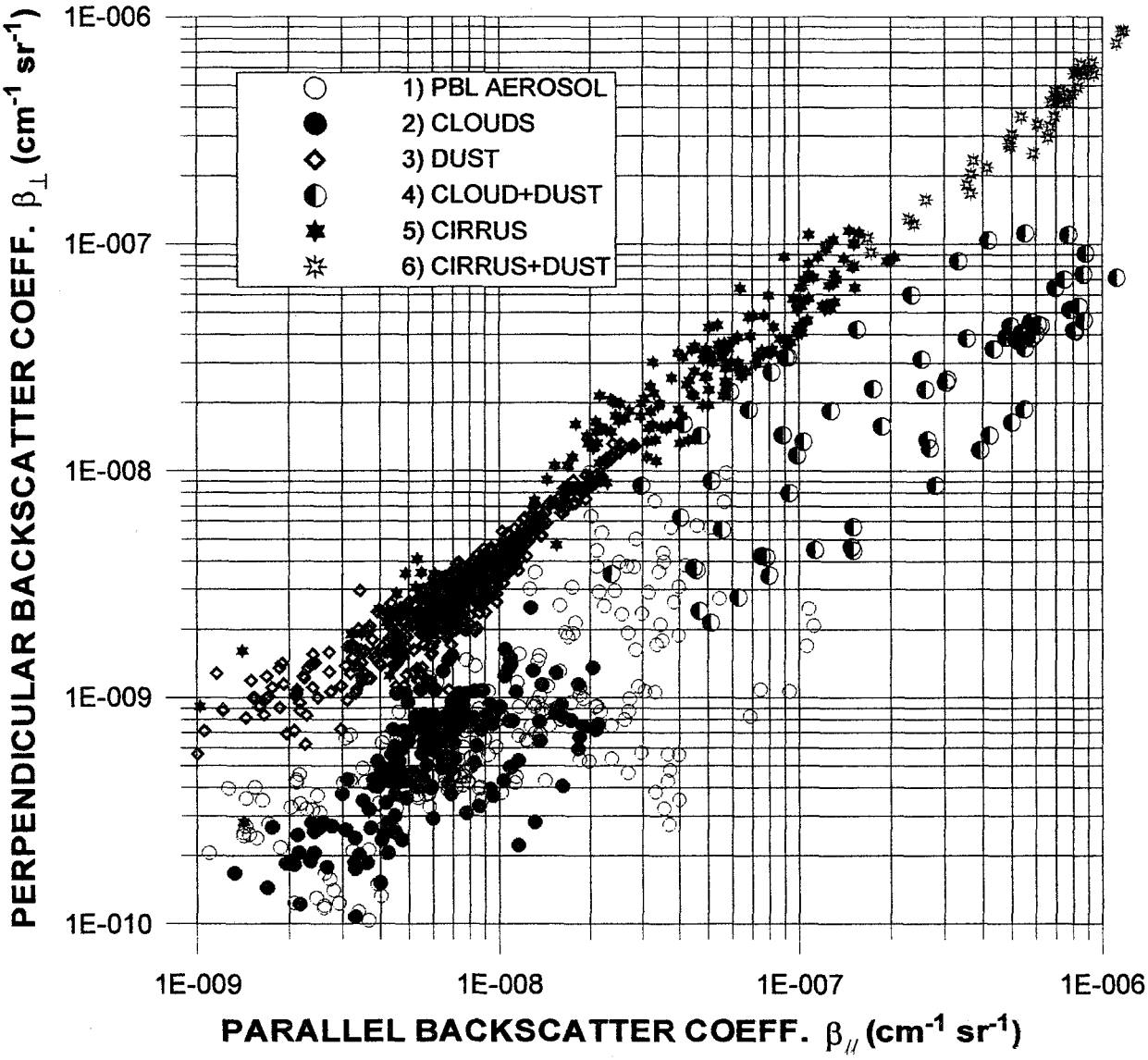

FIGURE 4. Perpendicular polarization coordinate analysis of the VELIS data collected at Crete (35N-23E), during the PAUR II campaign (May 5-25, 1999).

c\velis\data...crselecm.grf

LIDAR SIGNAL ANALYSIS

(VELIS-CNR; ch // ; 24-03-2001)
ROME TOR VERGATA (41.8N-12.6E)

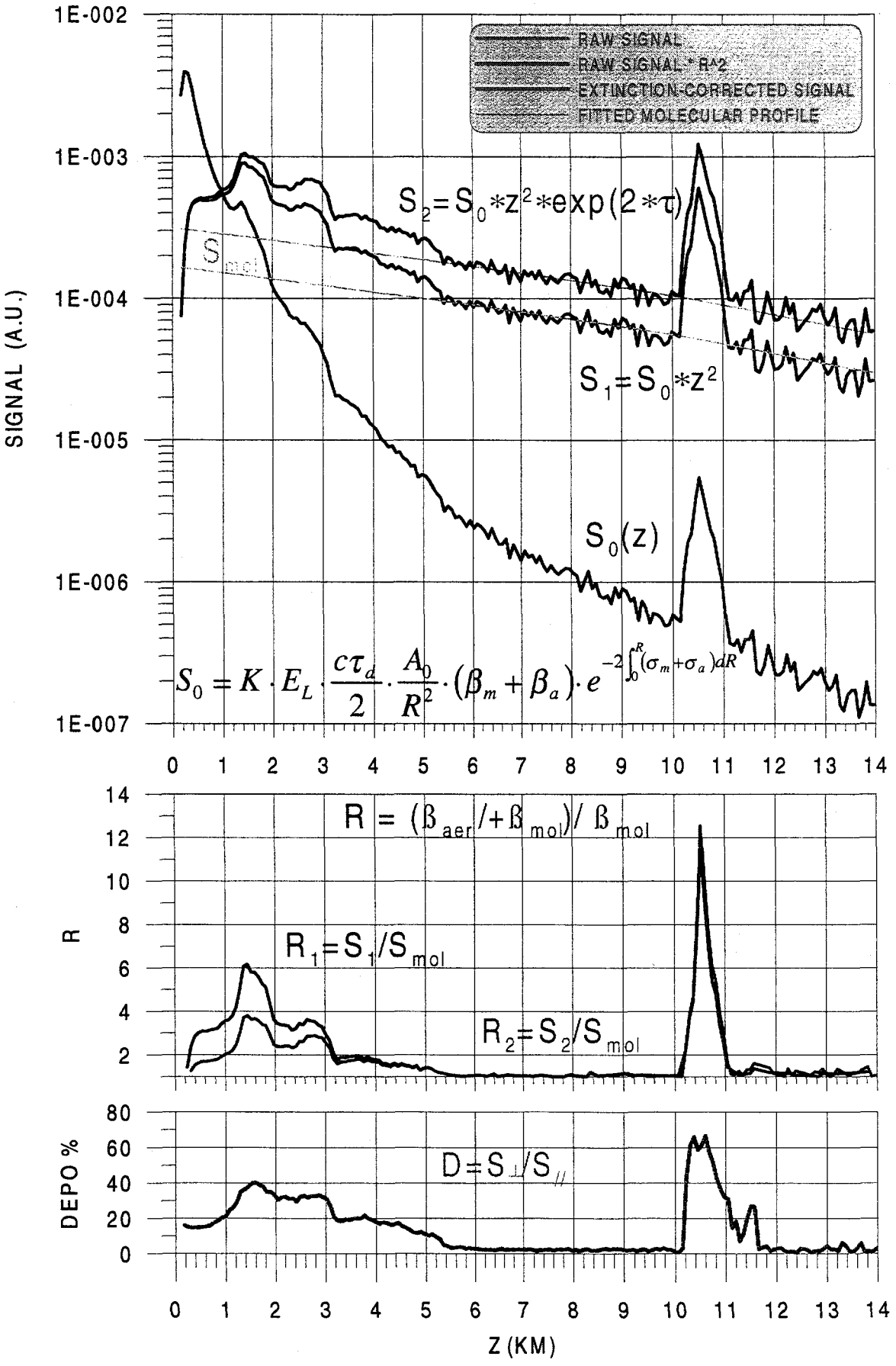

sgnl&eq.ppt
sgnlstep2.grf

Lognormal size-distribution:

$$\frac{dN_i(r)}{d\log r} = \frac{N_i}{\sqrt{2\pi}\log\sigma_i}\exp\left(-\frac{(\log r - \log r_{Mi})^2}{2(\log\sigma_i)^2}\right)$$

*MARITIME**	*Size-distribution*					*Refractive index*	
component	mode	parameter					
		$r_{Mi}(\mu m)$	σ_i	$N_i/N_{tot}(\%)$	$N_{tot}(cm^{-3})$	$m_{\Re e}$	$m_{\Im m}$
Sea-salt	1	0.05 - 0.1	1.4 - 2.03	5 - 70	500-800	1.5	$6.9\cdot10^{-9}$
	2	0.4 - 0.6	1.4 - 2.03	0.4 - 3.0			
sulfates	3	0.02 - 0.1	1.4 - 2.03	30 - 90		1.43	$1\cdot10^{-8}$

DUST	*Size-distribution*					*Refractive index*	
component	mode	parameter					
		$r_{Mi}(\mu m)$	σ_i	$N_i/N_{tot}(\%)$	$N_{tot}(cm^{-3})$	$m_{\Re e}$	$m_{\Im m}\cdot10^{-3}$
desert-dust	1	0.02-0.08	1.5 - 2.1	93 -98	200-1500	1.5 - 1.55	4 -8
	2	0.3 -1.5	1.5 - 2.0	2 - 7			

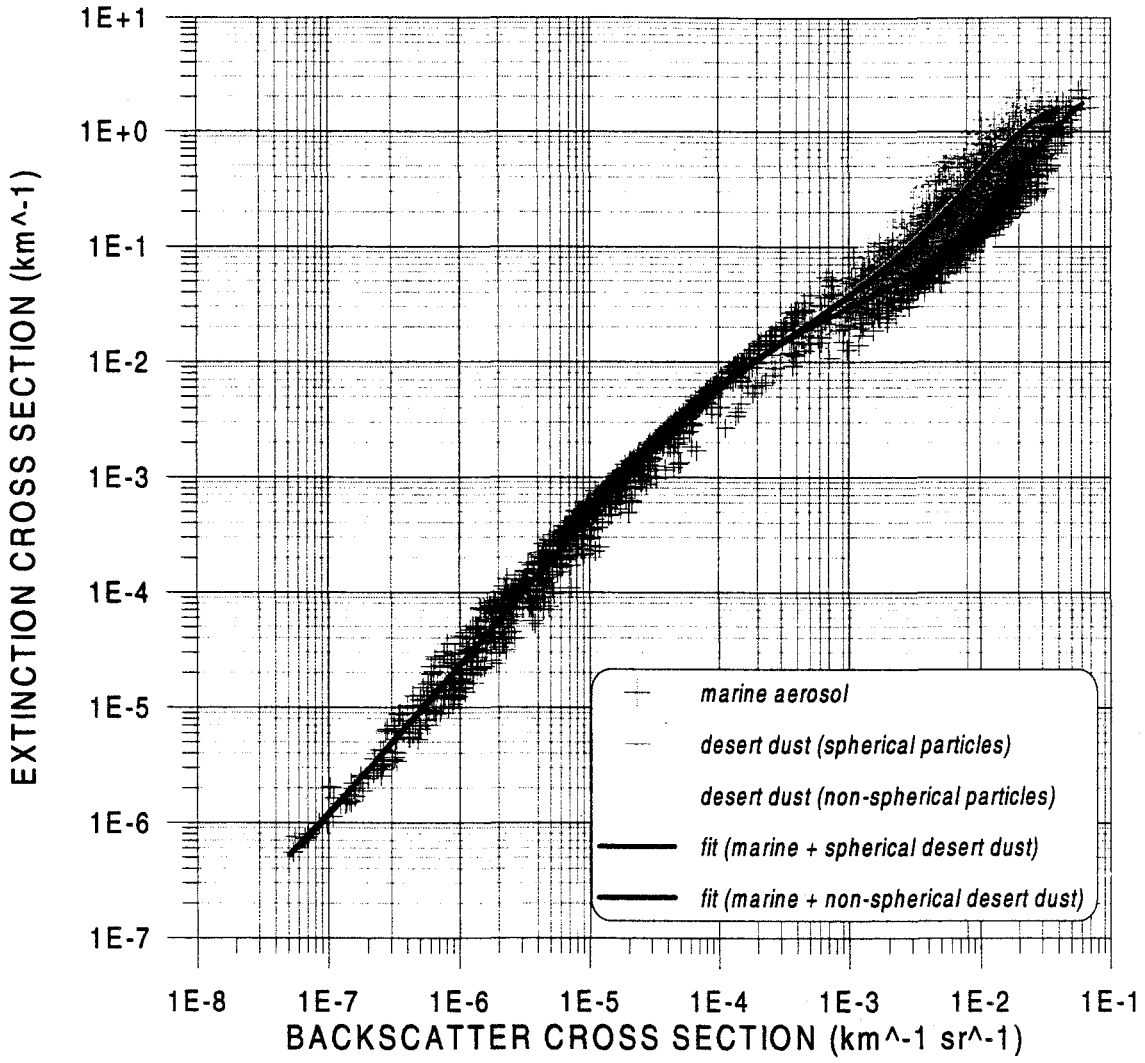

Extinction model output results for marine and desert-dust aerosols (plotted as function of backscattering) and fitted curves. Each curve has been obtained fitting 20.000 (marine) + 20.000 (desert-dust) points (1/20 plotted above).

Barnaba and Gobbi - JGR, 106, p3005, 2001

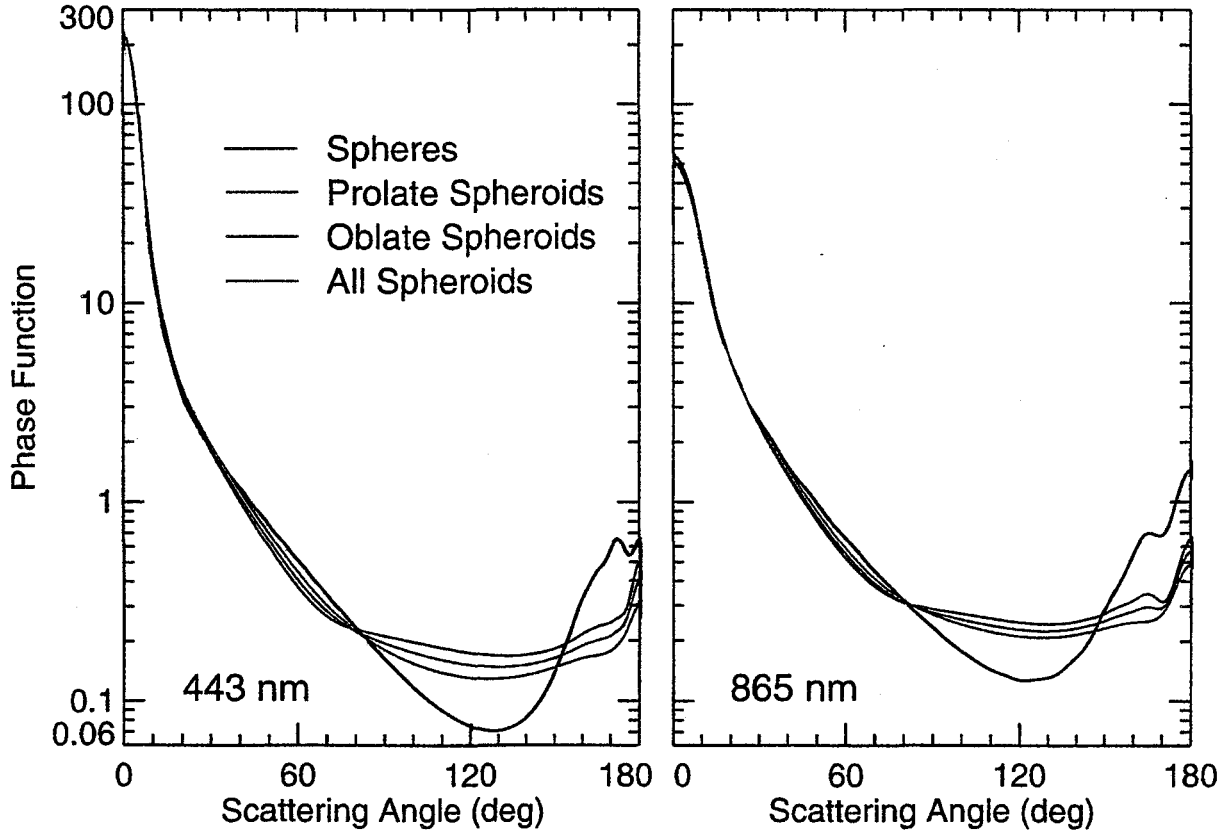

Plate 3. The upper panels demonstrate the effect of varying width of the spheroid aspect-ratio distribution and show ensemble-averaged phase functions for equiprobable shape mixtures of prolate and oblate spheroids with different aspect-ratio ranges. For all shape distributions the aspect-ratio step size is equal to 0.1. The lower panels show phase functions for polydisperse spheres and ensemble-averaged phase functions for equiprobable shape mixtures of prolate spheroids (green curve), oblate spheroids (blue curve), and prolate and oblate spheroids (red curve) with aspect ratios ranging from 1.2 to 2.4 in steps of 0.1. All curves were computed for the modified lognormal distribution of surface-equivalent-sphere radii corresponding to the accumulation mode of dustlike tropospheric aerosols (equation (9)) at wavelengths 443 and 865 nm. The spectral refractive indices are $1.53 + 0.0085i$ at 443 nm and $1.53 + 0.0012i$ at 865 nm.

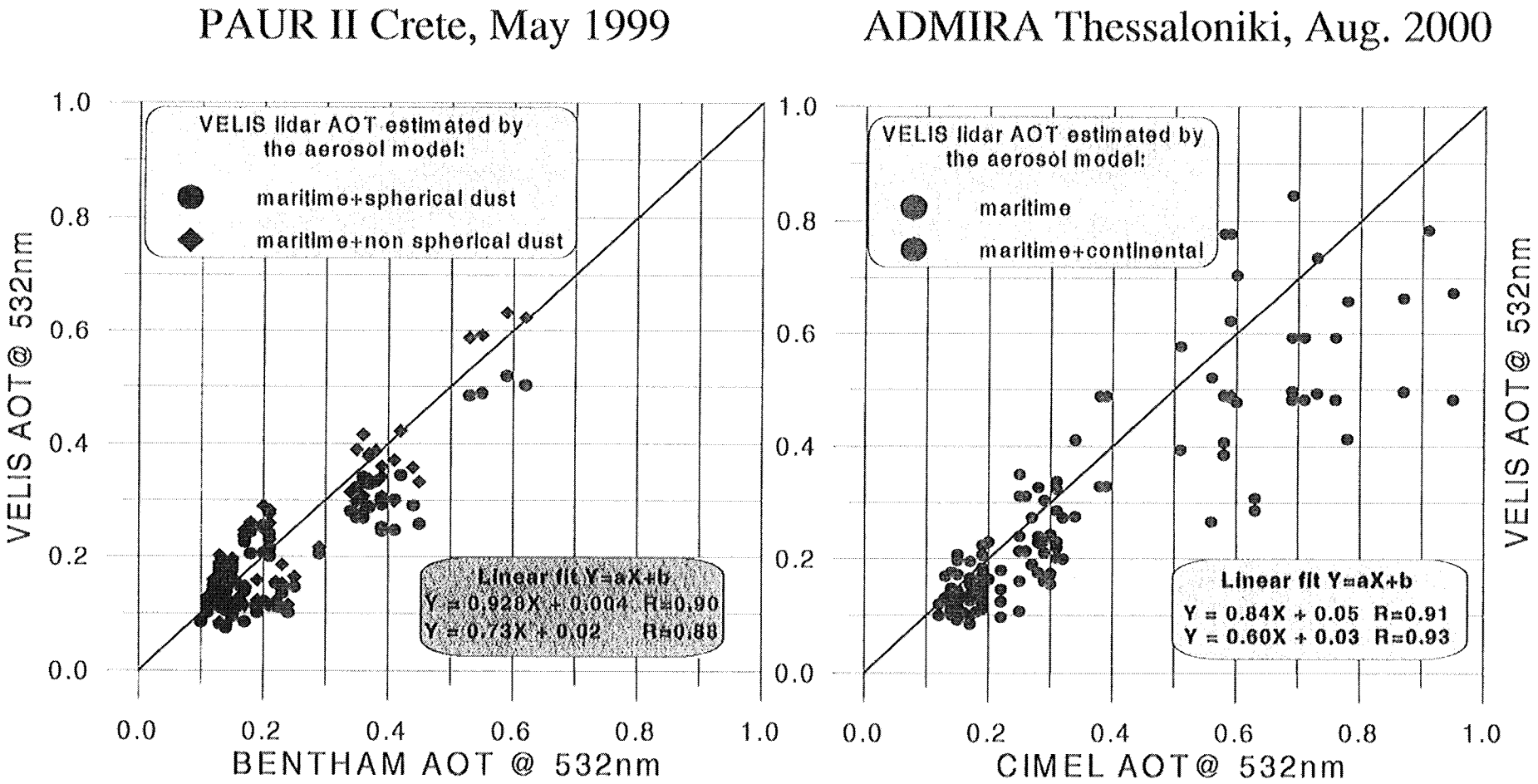
PAUR II Crete, May 1999
VELIS lidar AOT estimated by the aerosol model:
maritime+spherical dust
maritime+non spherical dust
Linear fit Y=aX+b
Y = 0,928X + 0,004 R=0,90
Y = 0,73X + 0,02 R=0,88
VELIS AOT @ 532nm
BENTHAM AOT @ 532nm
0.0
0.2
0.4
0.6
0.8
1.0
ADMIRA Thessaloniki, Aug. 2000
VELIS lidar AOT estimated by the aerosol model:
maritime
maritime+continental
Linear fit Y=aX+b
Y = 0.84X + 0.05 R=0.91
Y = 0.60X + 0.03 R=0.93
VELIS AOT @ 532nm
CIMEL AOT@ 532nm